Cellular and Molecular Biology
E-ISSN : 1165-158X / P-ISSN : 0145-5680
www.cellmolbiol.org

Effect of Glucocorticoid Nanoliposomes on Vascular Endothelial Growth Factor Expression in Brain Tissue of Rats with Tuberculous Meningitis

Xianyue Guan[1#], Chuanyang Dai[2#], Guannan Qin[2*]

[1] Department of Endocrinology, The Second Affiliated Hospital of Guizhou University of Traditional Chinese Medicine, Guiyang, 550003, China
[2] Department of Emergency, The Affiliated Hospital of Guizhou Medical University, Guiyang, 550004, China

#These authors contributed equally to this work as co-first author

ARTICLE INFO

Original paper

Article history:
Received: April 1, 2022
Accepted: August 5, 2022
Published: August 31, 2022

Keywords:

methylprednisolone sodium succinate, nanoliposomes, tuberculous meningitis (TBM), glucocorticoid, vascular endothelial growth factor (VEGF)

ABSTRACT

To investigate the effect of human brain-targeted nanoliposomes encapsulating methylprednisolone sodium succinate on the level of vascular endothelial growth factor (VEGF) in brain tissue of rats with tuberculous meningitis (TBM), the nanoliposome DSPE-^{125}I-AIBZM-MPS was prepared. 180 rats were divided into normal control, TBM infection, and TBM treatment groups. The brain water content, Evans blue (EB) content, VEGF, and the gene and protein expression of receptors (Flt-1, Flk-1) of rats after modeling were measured. The brain water content and EB content in the TBM treatment group were significantly lower than those in the TBM infection group at 4 and 7 days after modeling ($P < 0.05$). The expression of VEGF and its receptor Flt-1 mRNA in the brain tissue of rats in the TBM infection group was significantly higher than that in the normal control group at 1, 4, and 7 days after modeling ($P < 0.05$). The expression of VEGF and its receptor Flt-1 mRNA in the brain tissue of rats in the TBM treatment group was significantly higher than that in the TBM infection group at 1, 4, and 7 days after modeling ($P < 0.05$). In summary, the prepared DSPE-^{125}I-AIBZM-MPS nanoliposomes can effectively reduce brain water content and EB content and reduce the release of inflammatory factors of brain tissue in rats, playing a role in the treatment of TBM in rats by regulating the expression of VEGF and its receptor Flt-1 mRNA.

Doi: http://dx.doi.org/10.14715/cmb/2022.68.8.14

Introduction

Tuberculous meningitis (TBM) is a cerebrovascular disease caused by Mycobacterium tuberculosis. When tuberculosis occurs, Mycobacterium tuberculosis in the lesion will stay in the meninges, brain parenchyma, and other parts, constituting an insidious lesion. If the lesion ruptures, Mycobacterium tuberculosis will enter the subarachnoid cavity, resulting in tuberculous inflammation (1-3). This disease is the most important type of pediatric tuberculosis, which usually occurs within three months to one year after primary pulmonary tuberculosis infection and is more common in children aged 1 to 3 years. Before the introduction of anti-TB drugs, this rate was almost 100%. (4,5). At present, the understanding of the occurrence factors of TBM is not clear, which may be related to the high allergy of the body during primary tuberculosis in patients. From the pathogenesis point of view, TBM is secondary tuberculosis, so it is necessary to pay attention to finding the primary lesion (6-8). In recent years, with the development and popularization of bacillus Calmette-Guerin (BCG) vaccination and tuberculosis prevention and treatment, the incidence and mortality of TBM have been significantly reduced. If early detection and treatment can be performed, then most patients can be cured. Otherwise, there will still be a high mortality rate (9). Therefore, early diagnosis and reasonable treatment are the keys to improving the prognosis of this disease.

Current treatments for TBM include general treatment, adrenocorticotropic hormone application, and anti-TB treatment. General treatment is indicated for early cases, that is, hospitalization, bed rest, administration of nutrient-rich foods containing high vitamins and high protein to patients, and nasogastric feeding for comatose patients (10). Antituberculosis drugs generally use fungicides with strong penetration and high cerebrospinal fluid concentration, such as isoniazid, streptomycin, p-aminosalicylic acid, and rifampicin, but attention should be paid to the side effects of these drugs during use, such as hearing changes, visual changes, and liver function (11-13). Adrenocorticotropic hormone can effectively inhibit the inflammatory response and reduce arterial intimal inflammation and meningeal irritation signs, which is an effective adjuvant therapy to anti-TB drugs and is usually effective in the early application (14,15). Glucocorticoid is a kind of steroid hormone secreted by the bundle of the adrenal cortex. It is mainly cortisol. It has the function of regulating the biosynthesis and metabolism of sugar, fat, and protein. It also has the function of inhibiting immune response, anti-inflammatory, anti-toxic, and anti-shock. (16). As one of the important discoveries in the medical community in the 20th century, glucocorticoids are indispensable drugs in many departments and have an irreplaceable role. They are widely used in the treatment of TBM, but their efficacy and safety have been controversial (17).

Nanoliposome is a kind of liposome structure with a

* Corresponding author. Email: qinguannan2022@yandex.com

particle size less than 100 nm. It is a kind of ultramicro spherical carrier preparation formed by a lipid bilayer. It is a typical representative of a nano drug delivery system. It can effectively improve the solubility of encapsulated drugs and improve the therapeutic effect of drugs and has good biocompatibility (18,19). Therefore, human brain-targeted nanoliposomes DSPE-^{125}I-AIBZM-MPS encapsulating methylprednisolone sodium succinate were first prepared and characterized and compared with DSPE-MPS liposomes without markers, and then 180 Sprague-Dawley (SD) male rats were divided into normal control group, TBM infection group, and TBM treatment group, and the brain water content, Evans blue (EB) content, gene and protein expression levels of vascular endothelial growth factor (VEGF) and receptors (Flt-1, Flk-1), hematoxylin/eosin (HE) staining results of sections, and inflammatory factor levels of rats were measured after modeling to comprehensively evaluate the efficacy of glucocorticoid nanoliposomes in rats with TBM.

Materials and Methods

Experimental animals

180 SD male rats purchased from Shanghai Jake Biotechnology Co., Ltd. were selected as research samples, weighing 180 ± 10 g. Adaptive feeding was carried out one week before the experiment, and free drinking water and eating. The experiment was conducted according to the implementation rules of the Ministry of Health of the People's Republic of China on the management of medical laboratory animals (Order No. 55 of the Ministry of Health of January 25, 1998).

Preparation of human brain-targeted methylprednisolone nanoliposomes

Cholesterol, distearoylphosphatidylethanolamine-polyethylene glycol-carboxylic acid (DSPE-PEG2000 - Acid), distearoylphosphatidylethanolamine-polyethylene glycol (DSPE-PEG2000), and distearoylphosphatidlycholine (DSPC) were mixed in a certain proportion (molar ratio of materials), and then added into a mixed solvent of chloroform/methanol, and frozen overnight with nitrogen. The next day, 150 mmol of calcium acetate solution was used for hydration, an ultrasound bath for half an hour, then Avanti micro liposome extruder (Shanghai BenRo Chemical Co., Ltd.) was used about 15 times, and the obtained liposome suspension was dialyzed at 4℃ overnight. The pH gradient was established by remote control loading method, and methylprednisolone sodium succinate was loaded into liposomes and bathed at 65℃ for 30 min to obtain DSPE-MPS liposomes, which were stored at 4℃. Then, 50 μL 0.3 mol / L carbodiimide (EDC) and 50 μL 0.3 mol / L N-hydroxysuccinimide (NHS) were added, stirred at 25℃ for 15 min, neutralized with NaOH to pH 7.3. Finally, the formamide derivatives (^{125}I-AIBZM) were mixed with the activated nanoliposome suspension and stirred at 4℃ for 10 h to obtain the human brain-targeted nanoliposomes DSPE-^{125}I-AIBZM-MPS encapsulating methylprednisolone sodium succinate.

The free dose, total dose, actual package amount, and the amount of phospholipid in drug-loaded liposomes at different stages were measured by high-performance liquid chromatography (HPLC). The encapsulation rate and drug-to-lipid ratio were calculated. , .

$$Encapsulation\ rate = \frac{Total\ dose - Free\ dose}{Total\ dose} \times 100\%$$

$$Drug-to-lipid\ ratio = \frac{Actual\ package\ amount}{The\ amount\ of\ phospholipid\ in\ drug-loaded\ liposomes} \times 100\%$$

Preparation and intervention of nuclear meningitis rat model

According to different treatment methods, all rats were randomly divided into normal control group, TBM infection group, and TBM treatment group, with 60 rats in each group.

The rats in the TBM infection group and treatment group were injected with Mycobacterium tuberculosis suspension via tail vein, and the normal control group was injected with the same amount of normal saline. In the TBM infection group and TBM treatment group, Mycobacterium tuberculosis H37Rv, which was grown on a 7H9 medium for two weeks, was filtered, centrifuged, and dispersed to prepare the bacterial suspension with a concentration of 2.5 × 10^6 CFU / mL. Each rat was injected with 0.2 ml suspension/rat (bacterial amount: 5 × 10^5 CFU / rat) via tail vein and placed in a negative pressure environment (humidity: 55 ± 15 %, 21 ± 2℃). There was a cycle of 12 h light / 12 h dark. Animals could easily obtain food and water. The TBM model was formed after 14 days. After the formation of the TBM model, rats in the TBM treatment group were injected DSPE-^{125}I-AIBZM-MPS (4 mg/kg ·d) intraperitoneally, once every 24 h, until death. On the 1st, 4th, and 7th day after successful modeling, 20 rats in each group were sacrificed to observe the experimental indexes.

Determination of water content in rat brain tissue

On the 1st, 4th, and 7th day after the model was successfully established, 5 rats in each group were decapitated, the brains were removed as soon as possible, the left cerebral hemisphere was separated, and the blood stains on the brain surface were sucked out with filter paper, and placed in a weighed glass weighing cup with cover, and wet weigh was weighed with an electronic analytical balance (graduation value 0.1 mg). They were placed in a constant temperature drying oven at 110℃ for baking for 24-36 h to a constant weight (the difference between the two weighing samples was ≤ 0.2 mg), and dry weigh was weighed, and then the percentage of brain water content was calculated with Elliot equation.

$$Brain\ water\ content = \frac{Wet\ weight - Dry\ weight}{Wet\ weight} \times 100\%$$

EB content in rat brain tissue

On the 4th and 7th day after successful modeling, 5 rats in each group were injected with 2 % EB (2 mg/kg) via the tail vein 1 hour before sacrifice, anesthetized by intraperitoneal injection of 1 % pentobarbital sodium, and the hearts were rapidly opened to expose and perfused with 500 mL of normal saline at 37℃ to cause clear fluid outflow from the right atrial appendage. The content of EB in brain tissue was determined by the formamide digestion method: after measuring the wet weight of the cerebral cortex tissue samples, the samples were placed in the centrifuge tube containing formamide with 4 times the volume of samples. The centrifuge tube was covered, and samples were bathed at 5℃ for 24 h and centrifuged

at 1,500 r / min for 10 min. The supernatant was taken and the absorbance (A) value was measured at 635 nm of the maximum absorption spectrum of EB. The EB content was determined in the standard curve.

Detection of VEGF and receptor gene and protein expression in rat brain tissue

Ten rats in each group were anesthetized with 10 % chloral hydrate, the upper end of the cervical spine was clamped with a vertebral plate rongeur, the fur was removed, the rat skull was dissected, the vascular nerves and soft tissues were bluntly separated after brain exposure, the brain was removed and placed on an ice bag, and the hippocampal tissue was dissected out. 120 mg of brain slice cortex was stored in liquid nitrogen.

On days 4 and 7, after successful modeling: (1) the gene expression of VEGF and receptors (Flt-1, Flk-1) of brain tissue in the TBM infection group was detected by RT-PCR; (2) the protein expression level of VEGF and receptors of brain tissue in the TBM infection group was detected by Western blot.

Observation indexes

HE staining was performed on brain tissue sections from rats in each group. Avidin biotin complex-enzyme-linked immunosorbent assay (ABC-ELISA) was used to detect the expression levels of inflammatory factors (IL-6, IL-10, TNF-α, TGF-β) in rat brain tissue. Eight rats were anesthetized with 1 % chloral hydrate, and after removing the hair from the neck, four of them were injected with 150 μL DSPE-^{125}I-AIBZM-MPS and the other four were injected with 150 μL DSPE-MPS for intravital fluorescence imaging.

Statistical methods

The data was analyzed by SPSS 19.0 statistical software. The measurement data were expressed as mean ± standard deviation ($\bar{x}\pm s$), and the enumeration data were expressed as a percentage (%). One-way analysis of variance was used for pairwise comparisons. The difference was statistically significant at $P < 0.05$.

Results

Characterization of human brain-targeted methylprednisolone nanoliposomes

Figure 1 shows the transmission electron microscopy of DSPE-MPS nanoliposomes and DSPE-^{125}I-AIBZM-MPS nanoliposomes, and the two nanoliposomes have similar shapes and size, neat edges, regular shape, and good dispersity.

Figure 2 indicates the nanoliposome encapsulation rate and drug-to-lipid ratio. It was observed that the drug-to-lipid ratio of DSPE-MPS nanoliposomes was not significantly different from that of DSPE-^{125}I-AIBZM-MPS nanoliposomes ($P > 0.05$), while the encapsulation rate of DSPE-^{125}I-AIBZM-MPS nanoliposomes was significantly higher than that of DSPE-MPS nanoliposomes, and there was a significant difference ($P < 0.05$).

Intravital fluorescence imaging of rats

Figure 3 shows the intravital fluorescence imaging of DSPE-MPS nanoliposomes and DSPE-^{125}I-AIBZM-MPS nanoliposomes in rats. There was a strong fluorescence signal in the brains of rats injected with DSPE-^{125}I-AIBZM-MPS nanoliposomes, but no fluorescence signal in the brains of rats injected with DSPE-MPS nanoliposomes

Changes in brain water content in the three groups

Figure 4 suggests the changes in brain water content in the three groups. It showed that the brain water content in the TBM infection group was significantly higher than that in the normal control group on days 4 and 7 after modeling, and there was a significant difference ($P < 0.05$); in the brain water content in the TBM treatment group was significantly lower than that in the TBM infection group on days 4 and 7 after modeling, and there was a significant difference ($P < 0.05$).

Changes of EB content in brain tissue of three groups of rats

Figure 5A shows the EB standard curve, and its regression equation is y=14.339x-617, $R^2 = 0.9999$. Figure 5B shows the changes in EB content in the brain tissue of the three groups. It was found that the EB content in the brain tissue of rats in the TBM infection group was significantly higher than that in the normal control group on days 4 and 7 after modeling, and there was a significant difference ($P < 0.05$); the EB content in the brain tissue of rats in the TBM treatment group was significantly lower than that in

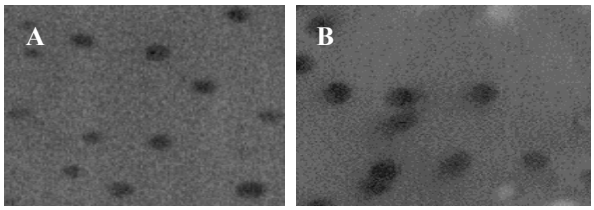

Figure 1. Transmission electron microscopy of nanoliposomes (200 nm). Note: A is DSPE-MPS nanoliposomes; B is DSPE-^{125}I-AIBZM-MPS nanoliposomes.

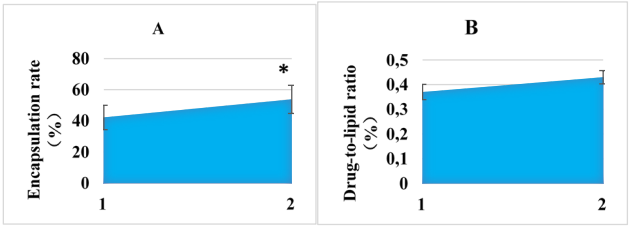

Figure 2. Entrapment rate of nanoliposomes and drug-to-lipid ratio. (1-2 for DSPE-MPS nanoliposomes, DSPE-^{125}I-AIBZM-MPS nanoliposomes, respectively). Note: A is the encapsulation rate; B is the drug-to-lipid ratio. * there was a statistically significant difference from 1 ($P < 0.05$).

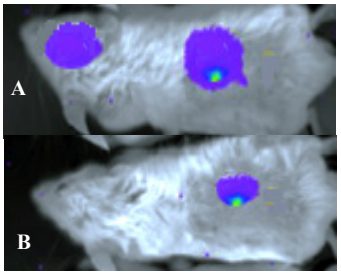

Figure 3. Transmission electron microscopy of nanoliposomes (200 nm). Note: A is DSPE-MPS nanoliposomes; B is DSPE-^{125}I-AIBZM-MPS nanoliposomes.

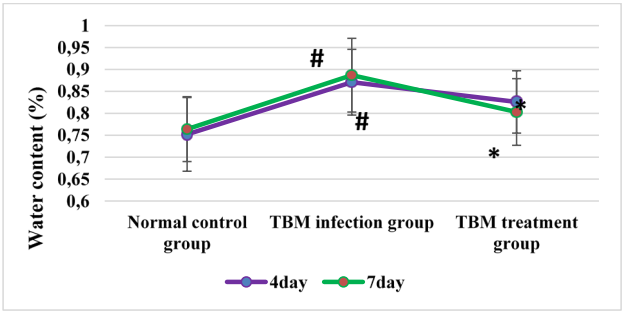

Figure 4. Changes in brain water content in three groups of rats. Note: * the difference was statistically significant compared with the TBM infection group (P<0.05); # the difference was statistically significant compared with the normal control group (P < 0.05).

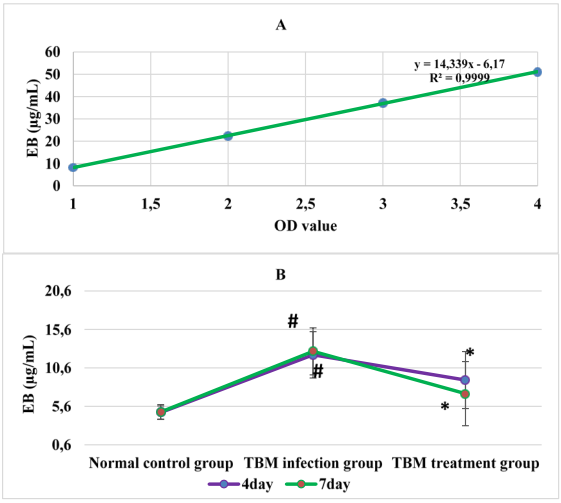

Figure 5. Changes of EB content in brain tissue of three groups of rats. Note: A is the EB standard curve; B is the content of EB in rat brains. * The difference was statistically significant compared with the TBM infection group (P < 0.05); # the difference was statistically significant compared with the normal control group (P < 0.05).

the TBM infection group on days 4 and 7 after modeling. There was a significant difference (P < 0.05).

HE staining of brain tissue of three groups of rats

Figure 6 reveals the HE staining diagram of the brain tissue of rats in the three groups. There was no vasodilation in brain tissue and no inflammatory cell infiltration in the subarachnoid space of rats in the normal control group; in the TBM infection group, there was obvious hyperemia in cerebral blood vessels, visceral pleural erosion, and many inflammatory cells around blood vessels; in TBM treatment group, there was mild hyperemia in cerebral blood vessels and a small amount of inflammatory cell infiltration around blood vessels.

Levels of inflammatory factors in brain tissue of rats in the three groups

Figure 7 shows the changes in the levels of inflammatory factors in the brain tissues of the three groups. The levels of IL-6, IL-10, TNF-α, and TGF-β in the brain tissues of rats in the TBM infection group were significantly higher than those in the normal control group on days 4 and 7 after modeling, and there was a significant difference (P<0.05); the levels of IL-6, IL-10, TNF-α, and TGF-β in the brain tissues of rats in the TBM treatment group were significantly lower than those in the TBM infection group

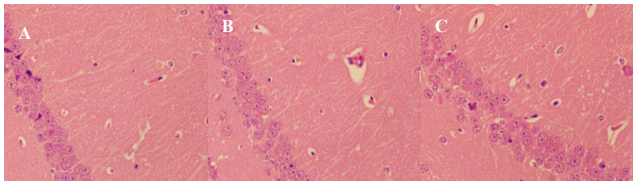

Figure 6. HE staining diagram of brain tissue of rats in the three groups (× 200). Note: A is the normal control group; B is the TBM infection group; C is the TBM treatment group.

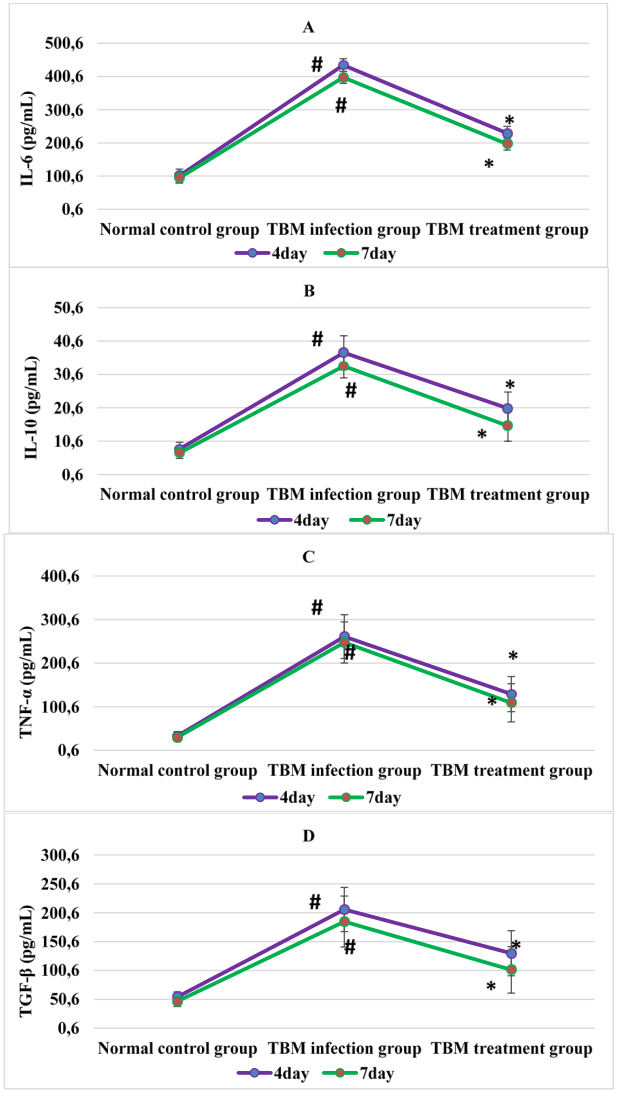

Figure 7. levels of inflammatory factors in brain tissue of three groups of rats. Note: A is IL-6; B is IL-10; C is TNF- α; D is TGF- β. * The difference was statistically significant compared with the TBM infection group (P<0.05); # the difference was statistically significant compared with the normal control group (P<0.05).

on days 4 and 7 after modeling. There was a significant difference (P < 0.05).

Expression levels of VEGF and its receptor mRNA in brain tissue of three groups of rats

Figure 8 shows the expression levels of VEGF and its receptor mRNA in the brain tissues of the three groups. The VEGF and its receptor Flt-1 mRNA levels in the brain tissues of rats in the TBM infection group were significantly higher than those in the normal control group on days 1, 4, and 7 after modeling, and there was a significant difference (P < 0.05). Flk-1 mRNA level in the TBM infection group was not statistically significant compared

with that in the normal control group on days 1, 4, and 7 after modeling (P>0.05). The level of VEGF and its receptor Flt-1 mRNA in the brain tissue of rats in the TBM treatment group was significantly decreased on days 1, 4, and 7 after modeling compared with that in the TBM infection group. There was a significant difference (P < 0.05), while the Flk-1 mRNA level was not statistically significant on days 1, 4, and 7 after modeling compared with that in the TBM infection group (P>0.05).

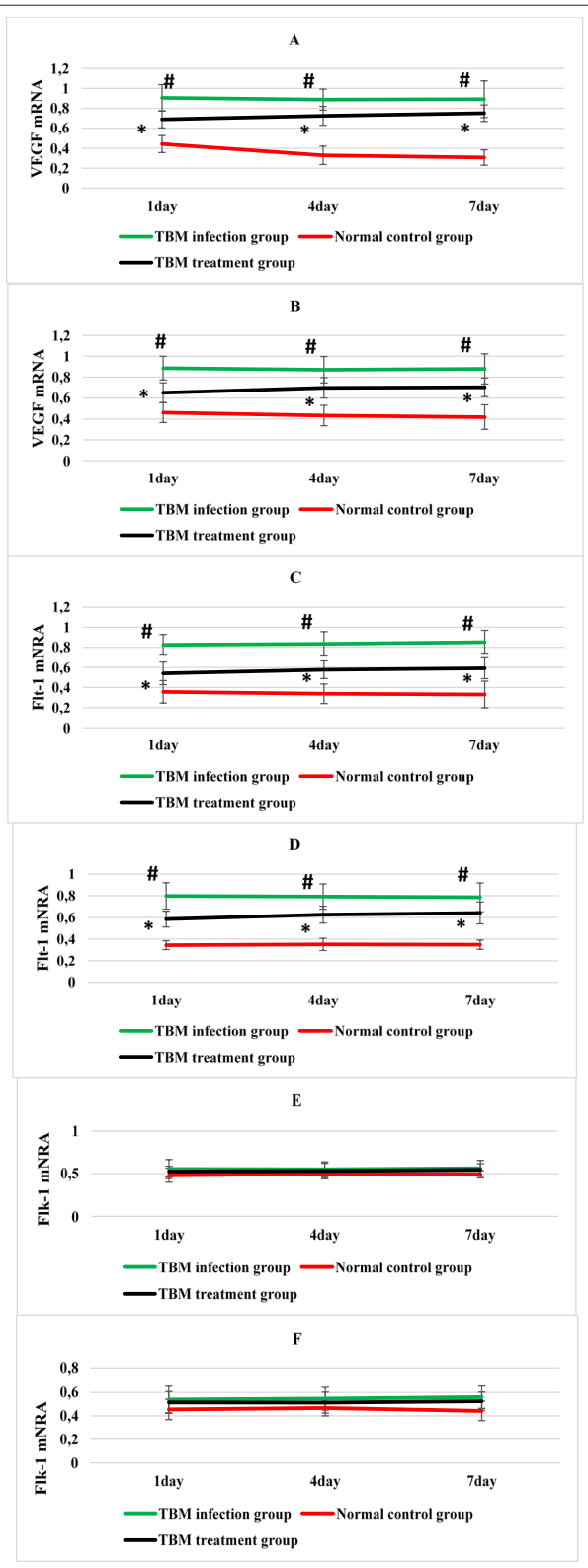

Figure 8. The expression level of VEGF and its receptor mRNA in brain tissue of rats in the three groups. Note: A and B are VEGF mRNA levels in cortex and hippocampus, respectively; C and D are Flt-1 mRNA levels in cortex and hippocampus, respectively; E and F are Flk-1 mRNA levels in cortex and hippocampus, respectively. * There was a statistically significant difference compared with the TBM infection group (P<0.05); # there was a statistically significant difference compared with the normal control group (P<0.05).

Expression levels of VEGF and its receptor protein in brain tissue of three groups of rats

Figure 9 shows the expression levels of VEGF and its receptor protein in the brain tissue of rats in the three groups. The expression levels of VEGF and its receptor Flt-1 protein in the brain tissue of rats in the TBM infection group were significantly higher than those in the normal control group on the 1st, 4th, and 7th day after modeling. There was a significant difference (P < 0.05). In contrast, the level of Flk-1 protein in the TBM infection group was not statistically significant compared with that in the normal control group on the 1st, 4th, and 7th day after modeling (P > 0.05). The expression levels of VEGF and its receptor Flt-1 protein in the brain tissue of rats in the TBM treatment group were significantly increased compared with those in the TBM infection group on days 1, 4, and 7 after modeling, and there was a significant difference (P < 0.05), while the Flk-1 protein levels were not significantly different from those in the TBM infection group on days 1, 4, and 7 after modeling (P > 0.05).

Discussion

The increasing incidence of TBM in recent years, coupled with complex clinical symptoms, long treatment times, and high drug resistance, makes the cure rate of patients very low and the prognosis very poor (20). The pathological changes of patients are also various, such as diffuse congestion of the meninges, flattening of the gyri, and a lot of thick gelatinous exudate appearing in subarachnoid space, and it is a hot topic for scholars to find more appropriate treatment from the pathogenesis (21,22). As a commonly used drug loading system in current research, nanoliposomes have the advantages of degradability, sustained release, and no immunogenicity. Therefore, human brain-targeted nanoliposomes DSPE-^{125}I-AIBZM-MPS encapsulating methylprednisolone sodium succinate were prepared and characterized and compared with DSPE-MPS liposomes without markers. It was found that the drug-to-lipid ratio of DSPE-MPS nanoliposomes was not significantly different from that of DSPE-^{125}I-AIBZM-MPS nanoliposomes (P > 0.05), while the entrapment rate was significantly higher than that of DSPE-MPS nanoliposomes, and there was a significant difference (P < 0.05). From the in vivo fluorescence imaging of rats, it was observed that there was a strong fluorescence signal in the brain of rats injected with DSPE-^{125}I-AIBZM-MPS nanoliposomes, but no fluorescence signal in the brain of rats injected with DSPE-MPS nanoliposomes, which indicated that the prepared nanoliposomes DSPE-^{125}I-AIBZM-MPS had significant brain targeting.

180 SD male rats were included as the study samples and divided into normal control group, TBM infection group, and TBM treatment group according to different intervention methods, with 60 rats in each group. The brain water content, EB content, gene and protein expression levels of VEGF and receptors (Flt-1, Flk-1), HE staining results of sections, inflammatory factor levels, and other indicators were measured after modeling. First, it was found that the brain water content of rats in the TBM

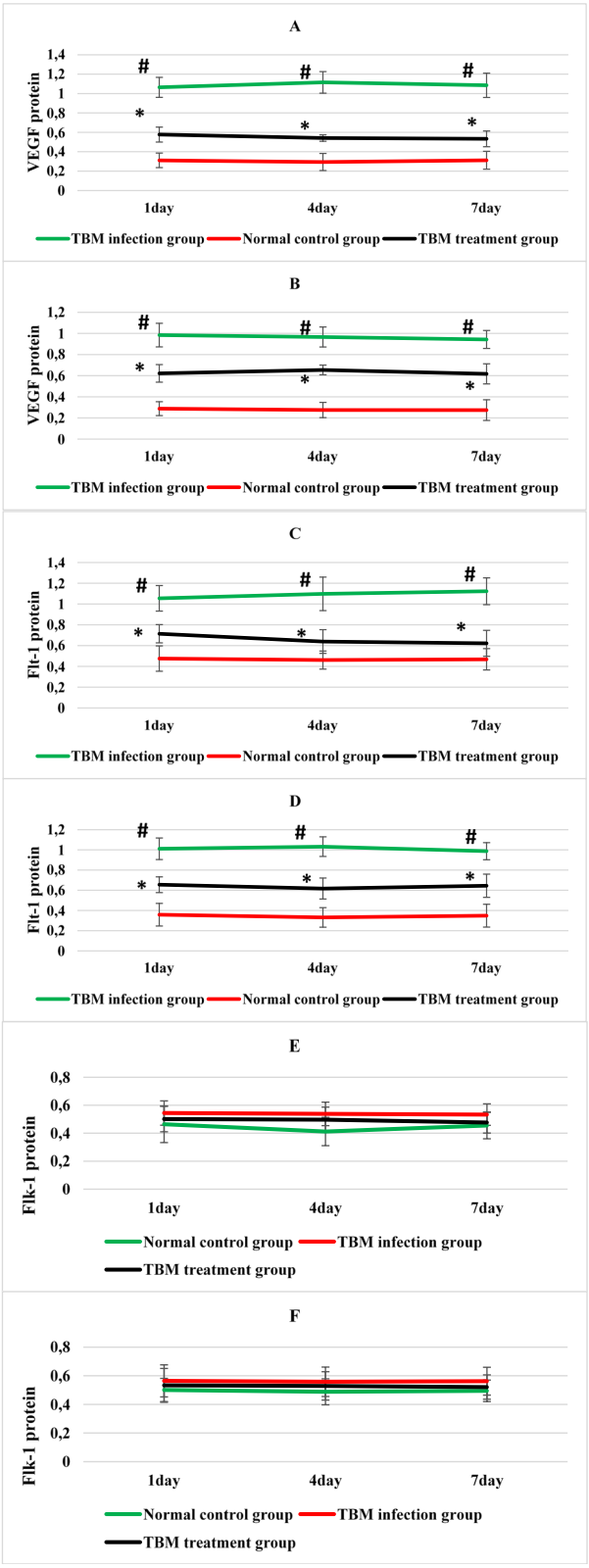

Figure 9. Expression levels of VEGF and its receptor protein in brain tissue of three groups of rats. Note: A and B are VEGF protein levels in cortex and hippocampus, respectively; C and D are the levels of Flt-1 protein in cortex and hippocampus, respectively; E and F are the levels of Flk-1 protein in cortex and hippocampus, respectively. * The difference was statistically significant compared with the TBM infection group (P<0.05); # the difference was statistically significant compared with the normal control group (P<0.05).

treatment group was significantly decreased on days 4 and 7 after modeling compared with that in the TBM infection group, and there was a significant difference (P < 0.05). When infected with tuberculosis bacteria, the cerebrovascular fluid and inflammatory substances in rats exuded out and entered the brain parenchyma, resulting in brain tissue cell edema, indicating that DSPE-^{125}I-AIBZM-MPS nanoliposomes could effectively improve the brain tissue cell edema and reduce the brain water content in the rat model (23). Analysis of the results of EB measurement showed that the EB content in the brain tissue of rats in the TBM treatment group was significantly decreased on days 4 and 7 after modeling compared with that in the TBM infection group, and there was a significant difference (P < 0.05). The higher EB content means stronger blood-brain barrier permeability and greater damage in rats, which shows that DSPE-^{125}I-AIBZM-MPS nanoliposomes can effectively alleviate the blood-brain barrier damage in rat models (24). From the results of inflammatory factors, the levels of IL-6, IL-10, TNF-α, and TGF-β in the brain tissue of rats in the TBM treatment group were significantly lower than those in the TBM infection group on days 4 and 7 after modeling, and there was a significant difference (P < 0.05), suggesting that DSPE-^{125}I-AIBZM-MPS nanoliposomes could effectively reduce the release of inflammatory factors in the brain tissue of rats and reduce the occurrence of inflammatory infection.

In addition, the changes of VEGF and its receptor mRNA expression in the brain tissue of rats were also analyzed. It was found that the expression levels of VEGF and its receptor Flt-1 mRNA in the brain tissue of the TBM infection group of rats were significantly higher than those in the normal control group on the 1st, 4th, and 7th day after modeling, and there was a significant difference (P < 0.05), which was similar to the results of Liao et al. (25). It may be due to the infiltration of inflammatory cells and the proliferation of endothelial cells in the pathogenesis of TBM, which led to stenosis of vascular lumen and hypoxia of brain tissue, and promoted the increase of VEGF and its receptor mRNA expression. The expression of VEGF and its receptor Flt-1 mRNA in the brain tissue of rats in the TBM treatment group was significantly higher than that of the TBM infection group on the 1st, 4th, and 7th day after modeling, and there was a significant difference (P < 0.05). VEGF is generally only expressed in a small amount of normal brain tissue. When infected with Mycobacterium tuberculosis, the expression level of VEGF is increased. Therefore, it speculates that DSPE-^{125}I-AIBZM-MPS nanoliposomes may regulate the expression level of VEGF and its receptor Flt-1 mRNA to play a role in the treatment of TBM in rats. The comparison results of VEGF and its receptor protein expression levels also confirm that.

The human brain-targeted nanoliposomes DSPE-^{125}I-AIBZM-MPS encapsulating methylprednisolone sodium succinate were prepared and compared with the DSPE-MPS liposomes without labels. Then, 180 SD male rats were divided into the normal control group, TBM infection group, and TBM treatment group according to different intervention methods, with 60 rats in each group. The brain water content, EB content, gene and protein expression levels of VEGF and its receptors (Flt-1, Flk-1), HE staining results of sections, and inflammatory factors were measured after modeling. It was found that the prepared DSPE-^{125}I-AIBZM-MPS nanoliposome had high brain targeting, which could effectively reduce the brain water content and EB content and reduce the release of inflammatory factors in rat brain tissue. It might play a role in the treatment of TBM rats by regulating the expression level

of VEGF and its receptor Flt-1 mRNA. However, there are still some shortcomings. The grouping of samples is relatively rough, and the glucocorticoid treatment group is not set. The data analysis on the safety of DSPE-^{125}I-AIBZM-MPS nanoliposomes is lacking, and the research samples will be re-included for further discussion. In conclusion, the results provide data reference for the pathogenesis and treatment of TBM.

Fundings

The research is supported by: Guizhou Science and Technology Foundation (Qiankehe Zhicheng (2017) 2881).

References

1. Donovan J, Figaji A, Imran D, Phu NH, Rohlwink U, Thwaites GE. The neurocritical care of tuberculous meningitis. Lancet Neurol. 2019 Aug;18(8):771-783. doi: 10.1016/S1474-4422(19)30154-1. Epub 2019 May 17. PMID: 31109897.
2. Méchaï F, Bouchaud O. Tuberculous meningitis: Challenges in diagnosis and management. Rev Neurol (Paris). 2019 Sep-Oct;175(7-8):451-457. doi: 10.1016/j.neurol.2019.07.007. Epub 2019 Aug 2. PMID: 31383464.
3. Marais S, Thwaites G, Schoeman JF, Török ME, Misra UK, Prasad K, Donald PR, Wilkinson RJ, Marais BJ. Tuberculous meningitis: a uniform case definition for use in clinical research. Lancet Infect Dis. 2010 Nov;10(11):803-12. doi: 10.1016/S1473-3099(10)70138-9. Epub 2010 Sep 6. PMID: 20822958.
4. Mezochow A, Thakur K, Vinnard C. Tuberculous Meningitis in Children and Adults: New Insights for an Ancient Foe. Curr Neurol Neurosci Rep. 2017 Sep 20;17(11):85. doi: 10.1007/s11910-017-0796-0. PMID: 28932979; PMCID: PMC5729589.
5. Mai NT, Thwaites GE. Recent advances in the diagnosis and management of tuberculous meningitis. Curr Opin Infect Dis. 2017 Feb;30(1):123-128. doi: 10.1097/QCO.0000000000000331. PMID: 27798497.
6. Garg RK. Microbiological diagnosis of tuberculous meningitis: Phenotype to genotype. Indian J Med Res. 2019 Nov;150(5):448-457. doi: 10.4103/ijmr.IJMR_1145_19. PMID: 31939388; PMCID: PMC6977359.
7. Garg RK, Sinha MK. Tuberculous meningitis in patients infected with human immunodeficiency virus. J Neurol. 2011 Jan;258(1):3-13. doi: 10.1007/s00415-010-5744-8. Epub 2010 Sep 17. PMID: 20848123.
8. Thwaites GE, van Toorn R, Schoeman J. Tuberculous meningitis: more questions, still too few answers. Lancet Neurol. 2013 Oct;12(10):999-1010. doi: 10.1016/S1474-4422(13)70168-6. Epub 2013 Aug 23. PMID: 23972913.
9. Garg RK, Malhotra HS, Gupta R. Spinal cord involvement in tuberculous meningitis. Spinal Cord. 2015 Sep;53(9):649-57. doi: 10.1038/sc.2015.58. Epub 2015 Apr 21. PMID: 25896347.
10. Shridhar A, Garg RK, Rizvi I, Jain M, Ali W, Malhotra HS, Kumar N, Sharma PK, Verma R, Uniyal R, Pandey S. Prevalence of primary immunodeficiency syndromes in tuberculous meningitis: A case-control study. J Infect Public Health. 2022 Jan;15(1):29-35. doi: 10.1016/j.jiph.2021.11.019. Epub 2021 Dec 2. PMID: 34883295.
11. Dhawan SR, Chatterjee D, Radotra BD, Vaidya PC, Vyas S, Sankhyan N, Singhi PD. A Child with Tuberculous Meningitis Complicated by Cortical Venous and Cerebral Sino-Venous Thrombosis. Indian J Pediatr. 2019 Apr;86(4):371-378. doi: 10.1007/s12098-018-2830-x. Epub 2019 Jan 9. PMID: 30623313.
12. van Toorn R, Solomons R. Update on the diagnosis and management of tuberculous meningitis in children. Semin Pediatr Neurol. 2014 Mar;21(1):12-8. doi: 10.1016/j.spen.2014.01.006. Epub 2014 Feb 2. PMID: 24655399.
13. Arzuaga JA, de la Fuente J, Tebas P, Pérez R, Masa C, Martínez J, de Letona ML. Meningitis tuberculosa en pacientes no infectados por VIH. Presentación de 21 casos [Tuberculous meningitis in patients without HIV infection. Presentation of 21 cases]. Enferm Infecc Microbiol Clin. 1992 Dec;10(10):576-80. Spanish. PMID: 1292598.
14. Yang Y, Qu XH, Zhang KN, Wu XM, Wang XR, Wen A, Li LJ. A Diagnostic Formula for Discrimination of Tuberculous and Bacterial Meningitis Using Clinical and Laboratory Features. Front Cell Infect Microbiol. 2020 Jan 17;9:448. doi: 10.3389/fcimb.2019.00448. PMID: 32010636; PMCID: PMC6978638.
15. Prévost MR, Fung Kee Fung KM. Tuberculous meningitis in pregnancy--implications for mother and fetus: case report and literature review. J Matern Fetal Med. 1999 Nov-Dec;8(6):289-94. doi: 10.1002/(SICI)1520-6661(199911/12)8:6<289::AID-MFM9>3.0.CO;2-H. PMID: 10582863.
16. Rowe JS, Shah SS, Marais BJ, Steenhoff AP. Diagnosis and management of tuberculous meningitis in HIV-infected pediatric patients. Pediatr Infect Dis J. 2009 Feb;28(2):147-8. doi: 10.1097/INF.0b013e318198d0b0. PMID: 19174688.
17. Woo SJ, Kim Y, Jung H, Lee JJ, Hong JY. Tuberculous Fibrosis Enhances Tumorigenic Potential via the NOX4-Autophagy Axis. Cancers (Basel). 2021 Feb 8;13(4):687. doi: 10.3390/cancers13040687. PMID: 33567693; PMCID: PMC7916030.
18. Opota O, Mazza-Stalder J, Greub G, Jaton K. The rapid molecular test Xpert MTB/RIF ultra: towards improved tuberculosis diagnosis and rifampicin resistance detection. Clin Microbiol Infect. 2019 Nov;25(11):1370-1376. doi: 10.1016/j.cmi.2019.03.021. Epub 2019 Mar 28. PMID: 30928564.
19. Arpinar Yigitbas B, Satici C, Kosar AF. Adenosine deaminase cutoff value when diagnosing tuberculous pleurisy in patients aged 40 years and older. Clin Respir J. 2021 Jan;15(1):109-115. doi: 10.1111/crj.13277. Epub 2020 Oct 6. PMID: 32970926.
20. Levi G, Rocchetti C, Mei F, Stella GM, Lettieri S, Lococo F, Taccari F, Seguiti C, Fantoni M, Natali F, Candoli P, Bortolotto C, Pinelli V, Mondoni M, Carlucci P, Fabbri A, Trezzi M, Vannucchi L, Bonifazi M, Porcarelli F, Gasparini S, Sica G, Valente T, Biondini D, Damin M, Liani V, Tamburrini M, Sorino C, Mezzasalma F, Scaramozzino MU, Pini L, Bezzi M, Marchetti GP. Diagnostic role of internal mammary lymph node involvement in tuberculous pleurisy: a multicenter study. Pulmonology. 2022 Feb 18:S2531-0437(22)00022-8. doi: 10.1016/j.pulmoe.2022.01.010. Epub ahead of print. PMID: 35190300.
21. Tong X, Lu H, Yu M, Wang G, Han C, Cao Y. Diagnostic value of interferon-γ-induced protein of 10kDa for tuberculous pleurisy: A meta-analysis. Clin Chim Acta. 2017 Aug;471:143-149. doi: 10.1016/j.cca.2017.05.034. Epub 2017 May 31. PMID: 28577960.
22. Li B, Lei Y, Hu Q, Li D, Zhao H, Kang P. Porous copper- and lithium-doped nano-hydroxyapatite composite scaffold promotes angiogenesis and bone regeneration in the repair of glucocorticoids-induced osteonecrosis of the femoral head. Biomed Mater. 2021 Sep 28;16(6). doi: 10.1088/1748-605X/ac246e. PMID: 34492640.
23. He T, Zhang C, Vedadghavami A, Mehta S, Clark HA, Porter RM, Bajpayee AG. Multi-arm Avidin nano-construct for intra-cartilage delivery of small molecule drugs. J Control Release. 2020 Feb;318:109-123. doi: 10.1016/j.jconrel.2019.12.020. Epub 2019 Dec 13. PMID: 31843642; PMCID: PMC7424591.
24. Fan K, Zeng L, Guo J, Xie S, Yu Y, Chen J, Cao J, Xiang Q, Zhang S, Luo Y, Deng Q, Zhou Q, Zhao Y, Hao L, Wang Z, Zhong L. Visualized podocyte-targeting and focused ultrasound responsive

glucocorticoid nano-delivery system against immune-associated nephropathy without glucocorticoid side effect. Theranostics. 2021 Jan 1;11(6):2670-2690. doi: 10.7150/thno.53083. PMID: 33456566; PMCID: PMC7806481.

25. Liao S, Wu J, Li Z, Cheng G, Lu B, Liu G, Li X, Lu W. Study on the Mechanism of Targeted Poly(lactic-coglycolic acid) Nano-Delivery Carriers in the Treatment of Hemangiomas. J Nanosci Nanotechnol. 2021 Feb 1;21(2):1236-1243. doi: 10.1166/jnn.2021.18689. PMID: 33183467.